# Conformations, Structures, and Vibrational Spectra of Triethylchloro- and Triethylbromosilane Using Theoretical Methods, Gas Phase Electron Diffraction, and IR and Raman Spectroscopy

**Manuel Montejo,[†] Derek A. Wann,[‡] Francisco Partal Ureña,[†] Fernando Márquez,[†] David W. H. Rankin,*[,‡] and Juan Jesús López González*[,†]**

*Physical and Analytical Chemistry Department, University of Jaén, Campus Las Lagunillas, E-23071, Jaén, Spain, and School of Chemistry, University of Edinburgh, West Mains Road, Edinburgh, United Kingdom EH9 3JJ*

*Received: October 10, 2006; In Final Form: February 16, 2007*

Conformational studies of triethylchlorosilane (TECS) and triethylbromosilane (TEBS) and the elucidation of their gas phase molecular structures have been accomplished by the combined use of theoretical (ab initio and density functional theory) calculations and experimental data from gas phase electron diffraction experiments. Additionally, analysis of the experimental features observed in the IR and Raman spectra recorded for both compounds has allowed us to propose a complete description of the vibrational spectra of both compounds, including an explanation of certain bands, which can only be correctly assigned when more than one conformer is considered to be present.

## Introduction

Organohalosilanes are an important family of compounds with a wide range of applications in organic and organometallic synthesis.[1] For instance, alkylhalosilanes are important precursors of alkylsilanols, which are well-known intermediates in industrially important sol−gel processes using organometallic compounds.[2] Following a series of previous studies dealing with the molecular structures and vibrational spectra of a number of trimethylsilane derivatives,[3−6] we carry out a joint theoretical and experimental study of the molecular structures and vibrational spectra of two related triethylsilylhalo derivatives, namely triethylchlorosilane (TECS) and triethylbromosilane (TEBS). Few works in the literature deal with the vibrational spectra of the title molecules.[7,8] In those that do, both TECS and TEBS are treated as symmetric top rotators belonging to the $C_{3v}$ symmetry group. From a structural point of view, there is only one previous work in which Volkov et al. report the microwave spectrum of triethylchlorosilane.[9]

The presence of three rotating ethyl groups makes it likely that there will be more than one minimum on the potential energy surfaces of TECS and TEBS. As such, the first task of this work was to perform a conformational study on both systems based on the calculated populations obtained by the application of the Boltzmann distribution equation and the data from the gas phase electron diffraction (GED) experiments. Thereafter, the multiconformer molecular structures of both compounds have been determined using a combination of experimental data from the GED experiments and the results from theoretical ab initio (RHF, MP2) and density functional theory (DFT, B3LYP) calculations. Finally, the IR and Raman spectra of TECS and TEBS have been recorded. These data, and those from theoretical calculations using the B3LYP method, have been employed to determine a complete vibrational assignment for both molecules.

## Experimental Section

Samples of TECS (purity >99%) and TEBS (purity ≥97%) were purchased from Sigma-Aldrich and used without further purification.

**Gas Phase Electron Diffraction.** Data were collected for TECS and TEBS using the Edinburgh GED apparatus.[10] An accelerating voltage of around 40 kV was used, representing an electron wavelength of approximately 6.0 pm. Scattering intensities were recorded on Kodak electron image films at nozzle-to-film distances of 127.81 and 284.12 mm for TECS and 92.26 and 258.61 mm for TEBS. Sample and nozzle temperatures were held at 293 K in the case of TECS, whereas for TEBS the sample and nozzle temperatures were 335 and 342 K, respectively, for the shorter distance and 313 and 323 K for the longer distance. The differences between the nozzle-to-film distances used for TECS and TEBS correspond to the necessary use of different ports for the room-temperature and high-temperature nozzles.

The weighting points for the off-diagonal weight matrices,[11] correlation parameters, scaling factors, and nozzle-to-film distances for both TECS and TEBS are given in Table S1 (Supporting Information). Also included are the electron wavelengths as determined from the scattering patterns for benzene, which were recorded immediately before or after the patterns for the sample compounds. The scattering intensities were measured using an Epson Expression 1680 Pro flatbed scanner and converted to mean optical densities as a function of the scattering variable, $s$, using an established program.[12] The data reduction and least-squares refinement processes were carried out using the ed@ed program[11] employing the scattering factors of Ross et al.[13]

**IR and Raman Spectroscopy.** IR spectra were recorded in the 300−4000 $cm^{-1}$ range for both TECS and TEBS in the

* Corresponding authors. E-mail: jjlopez@ujaen.es; d.w.h.rankin@ed.ac.uk.
[†] University of Jaén.
[‡] University of Edinburgh.

10.1021/jp0666481 CCC: $37.00 
Published on Web 03/28/2007

liquid and gaseous phases using a Fourier transform (FT) IR Bruker Vector 22 spectrophotometer, equipped with a Globar source and a deuterated triglycine sulfate detector, using standard cells for liquid and gas (10 cm path length), both equipped with CsI windows. All spectra were obtained at room temperature with a resolution of 1.0 $cm^{-1}$ and 100 scans.

The Raman spectra in the liquid phase of the samples were recorded with a Bruker RF100/S FT−Raman spectrometer, equipped with a Nd:YAG laser (excitation line 1064 nm, 600 mW of laser power) and a cooled Ge detector at liquid nitrogen temperature, using a standard liquid cell. The spectra were again recorded with a resolution of 1.0 $cm^{-1}$ and 100 scans.

**Computational Details.** All molecular orbital and DFT calculations reported in this work were performed using the Gaussian 03 program package.[14] Geometry optimizations for TECS and TEBS were carried out using MP2 and B3LYP methods, each with three different basis sets, namely, the standard split-valence 6-31G*,[15] the so-called DZP+diff described elsewhere,[16] and the augmented correlation-consistent double-zeta basis set of Dunning (aug-cc-pVDZ).[17]

For each of the conformers identified for each compound, an RHF/6-31G* force field was calculated, providing accurate amplitudes of vibration and vibrational correction terms for use in the GED refinement. The SHRINK program[18] was used to obtain corrections based on a curvilinear representation of the atomic motions.

For the vibrational study, frequency calculations were performed at the B3LYP level with 6-31G* and DZP+diff basis sets. To achieve a better understanding of the PED matrices, and in order to implement the scaled quantum mechanics force field (SQMFF) methodology,[19−21] the Cartesian force fields were transformed into more appropriate sets of so-called natural coordinates,[19] listed in Table S2 (Supporting Information). Some examples of the internal coordinates used for the natural-coordinate definitions are shown in Figure S1.

Following the SQMFF methodology, the quadratic force constants were scaled according to $F'_{ii} = \lambda_i F_{ii}$ and $F'_{ij} = (\lambda_i \lambda_j)^{1/2} F_{ij}$, where $F_{ii}$ and $F_{ij}$ are the quadratic quantum mechanically computed force constants, and $F'_{ii}$ and $F'_{ij}$ are the scaled equivalents. ($\lambda_i$ and $\lambda_j$ are the scaling factors.) The scaling factors (associated with the force constants expressed in natural coordinates) have been refined for the main conformer of each compound (taking 1.000 as the starting value) during the linear root-mean-square fitting of the theoretical frequencies to those observed experimentally. The scaling factors obtained for the main conformer were then transferred directly to the remaining conformers in order to predict their vibrational spectra. The force-field transformations, refinement of scaling factors, and normal-mode analyses were performed using the MOLVIB program.[22]

## Results and Discussion

**Theoretical Conformational Analysis.** Searches for conformers of TECS and TEBS were performed by rotating the three ethyl groups. These can adopt either gauche (*g*) or anti (*a*) orientations with respect to the Si−X (X = Cl, Br) bond. The presence of eclipsed conformations has been discounted as these would have much higher energies.

Five conformers were identified as real minima on the potential energy surfaces of both TECS and TEBS, with no imaginary frequencies for the calculations performed at the MP2/6-31G* level. The five conformers can be defined as follows: conformer I ($g^+g^+g^+$) has $C_3$ symmetry, with the three ethyl groups in gauche positions with respect to the Si−X bond, and conformer II ($ag^-g^+$) has $C_s$ symmetry. The remaining conformers have $C_1$ symmetry, that is, conformer III ($aag^+$), conformer IV ($ag^+g^+$), and conformer V ($g^+g^+g^-$). A $C_{3v}$ symmetric (*aaa*) conformation was calculated to have one imaginary frequency, which described one of the three Si−C torsions. As such, the *aaa* conformation is not a real structure, rather a transition state on the way to conformer III.

**TABLE 1: Relative Energies (kJ $mol^{-1}$) of the Five Conformers Defined for Each of TECS and TEBS, Calculated at All Levels Used in the Present Work**

| | | $\Delta G$, kJ $mol^{-1}$ | | | | |
|---|---|---|---|---|---|---|
| method | basis set | I | II | III | IV | V |
| | | Triethylchlorosilane | | | | |
| B3LYP | 6-31G* | 2.85 | 0.00 | 3.12 | 0.27 | 2.03 |
| | DZP+diff | 2.65 | 0.00 | 3.06 | 0.41 | 2.27 |
| | aug-cc-pVDZ | 2.70 | 0.00 | 3.60 | 0.21 | 1.80 |
| MP2 | 6-31G* | 2.92 | 0.00 | 3.71 | 0.87 | 4.40 |
| | DZP+diff | 3.55 | 0.00 | 3.90 | 0.89 | 4.82 |
| | aug-cc-pVDZ | 3.44 | 0.00 | 3.99 | 0.91 | 4.14 |
| | | Triethylbromosilane | | | | |
| B3LYP | 6-31G* | 2.59 | 0.00 | 3.84 | 0.44 | 2.20 |
| | DZP+diff | 2.71 | 0.00 | 3.33 | 0.58 | 2.92 |
| | aug-cc-pVDZ | 2.93 | 0.00 | 3.73 | 0.55 | 2.47 |
| MP2 | 6-31G* | 2.82 | 0.00 | 4.05 | 0.75 | 3.67 |
| | DZP+diff | 3.27 | 0.00 | 4.44 | 0.92 | 4.59 |
| | aug-cc-pVDZ | 2.97 | 0.00 | 4.49 | 0.91 | 3.69 |

**TABLE 2: Boltzmann Populations (%) for the Five Conformers of TECS and TEBS**

| | | population (%) | | | | |
|---|---|---|---|---|---|---|
| method | basis set | I | II | III | IV | V |
| | | Triethylchlorosilane | | | | |
| B3LYP | 6-31G* | 5.0 | 21.7 | 13.7 | 39.2 | 20.4 |
| | DZP+diff | 5.6 | 22.4 | 14.4 | 38.4 | 19.3 |
| | aug-cc-pVDZ | 5.3 | 21.5 | 11.3 | 39.8 | 22.1 |
| MP2 | 6-31G* | 6.3 | 28.0 | 14.2 | 40.6 | 11.0 |
| | DZP+diff | 5.2 | 29.2 | 13.8 | 42.0 | 9.8 |
| | aug-cc-pVDZ | 5.3 | 28.5 | 13.0 | 40.8 | 12.3 |
| | | Triethylbromosilane | | | | |
| B3LYP | 6-31G* | 5.9 | 23.1 | 11.2 | 39.3 | 20.5 |
| | DZP+diff | 5.9 | 24.3 | 14.1 | 39.2 | 16.5 |
| | aug-cc-pVDZ | 5.4 | 24.0 | 12.1 | 39.2 | 19.3 |
| MP2 | 6-31G* | 6.3 | 27.0 | 12.0 | 40.9 | 13.8 |
| | DZP+diff | 5.9 | 29.6 | 11.5 | 42.2 | 10.8 |
| | aug-cc-pVDZ | 6.3 | 28.3 | 10.7 | 40.3 | 14.4 |

The relative Gibbs free energies ($\Delta G$, kJ $mol^{-1}$) calculated for each of the five conformers using MP2 and B3LYP methods with 6-31G*, DZP+diff, and aug-cc-pVDZ basis sets are reported in Table 1 for both TECS and TEBS. Both the B3LYP and the MP2 methods calculate conformer II to be the global minimum.

The Boltzmann distribution equation has been used to take into account the relative multiplicities of the conformers based on the symmetry each possesses. When the Boltzmann equation distribution is implemented (using $T = 293$ K for TECS and $T = 323$ K for TEBS), both levels of calculation agree that conformer IV will have the highest population in the gas phase for both TECS and TEBS. As can be seen in Table 2, the calculated amounts of each conformer are quite similar when results from different methods are compared and also when TECS and TEBS are compared. Figure 1 compares the calculated (MP2/aug-cc-pVDZ) populations (in %) for the five conformers defined for both TECS and TEBS. Conformer IV (40.8% of TECS and 40.3% of TEBS) and conformer II (28.5% of TECS and 28.3% of TEBS) are calculated to be present in higher proportions than the remaining three conformers. The molecular structures and atom numbering for II and IV are

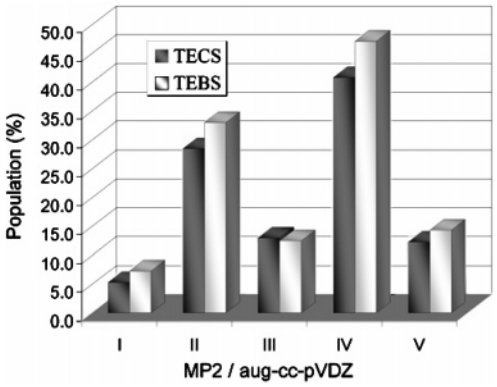


**Figure 1.** Graphical representation of the Boltzmann populations of the five conformers (MP2/aug-cc-pVDZ) for TECS and TEBS.

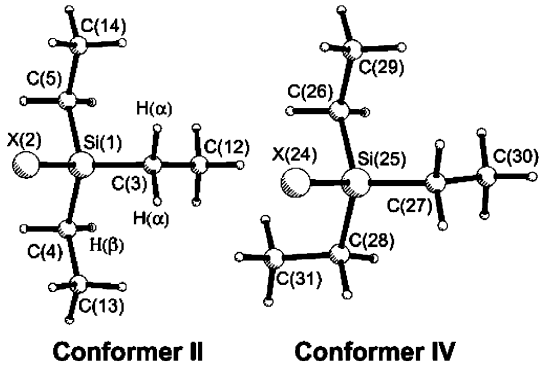


**Figure 2.** Molecular structures and atom numbering for the two main conformers of TECS (X = Cl) and TEBS (X = Br).

presented in Figure 2. The sum of the amounts of conformers II and IV is approximately 70% of the total composition of each sample in the gas phase.

**GED Study.** A model, composed of geometrical parameters and containing the two conformers being studied, was written for TECS. An almost identical model was used in the refinement of TEBS, except that any parameters relating to chlorine were replaced by ones that substituted bromine.

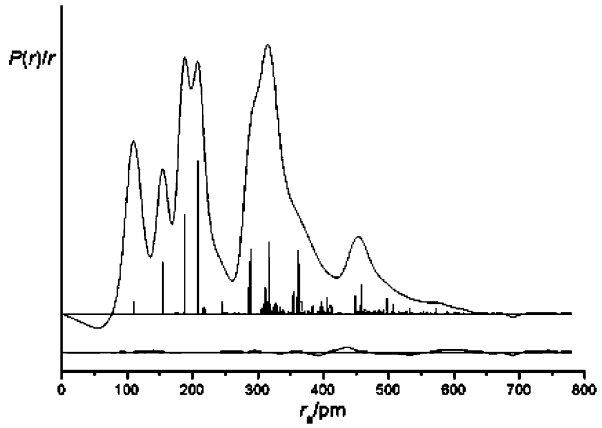


**Figure 3.** Experimental and difference (experimental − theoretical) radial-distribution curves $P(r)/r$ for TECS. Before Fourier inversion, the data were multiplied by $s\cdot\exp(-0.00002s^2)/(Z_{Cl} - f_{Cl})(Z_C - f_C)$.

As can be seen in Tables S3 and S4 (Supporting Information), which list the calculated geometries of all the conformers at all levels of calculation, only small differences in parameters values are found depending on the method and on the basis set for both TECS and TEBS. Furthermore, the range of values for any parameter throughout the different conformers is quite small. This has allowed us to model the two conformers using the same set of 11 parameters. The only exception was the requirement for one extra torsional parameter ($p_{12}$), X(24)−Si(25)−C(27)−C(30) (X = Cl, Br), for conformer IV. The 11 common parameters have as their starting points the average values calculated for the two conformers (MP2/aug-cc-pVDZ). Where differences exist in parameter values between conformers II and IV and the average values, these have been represented using fixed (i.e., non-refineable) differences, set at values determined from the MP2/aug-cc-pVDZ geometry optimizations.

Parameters 1−11 comprise four distances, namely, $r$Si−X ($p_1$), the mean $r$C−H distance ($p_2$), $r$C−C ($p_3$), and $r$C−Si ($p_4$). Four angle parameters were used: ∠X−Si−C ($p_5$), ∠Si−C−C ($p_6$), the average of the two ethyl ∠H−C−Si ($p_7$), and the

**TABLE 3: Refined and Calculated Geometric Parameters with Ab Initio Values and Restraints for TECS (X = Cl) and TEBS (X = Br) from the GED Study (Distances in Picometers and Angles in Degrees)**

| parameter descriptions | | triethylchlorosilane | | | triethylbromosilane | | |
|---|---|---|---|---|---|---|---|
| | | GED ($r_{h1}$) | MP2/aug-cc-pVDZ[a] | restraint | GED ($r_{h1}$) | MP2/aug-cc-pVDZ[a] | restraint |
| | | | Independent | | | | |
| $p_1$ | $r$Si−X | 208.6(1) | 212.2 | | 225.9(1) | 227.9 | |
| $p_2$ | $r$C−H | 110.6(1) | 110.2 | | 110.3(1) | 110.2 | |
| $p_3$ | $r$C−C | 154.5(1) | 154.2 | | 154.0(1) | 154.1 | |
| $p_4$ | $r$Si−C | 187.3(1) | 188.8 | | 187.2(1) | 188.9 | |
| $p_5$ | ∠X−Si−C | 106.7(1) | 107.0 | | 107.3(1) | 106.9 | |
| $p_6$ | ∠Si−C−C | 114.0(1) | 113.1 | | 116.0(1) | 113.1 | |
| $p_7$ | ∠H−C−Si | 109.2(4) | 108.1 | 1.0 | 110.0(5) | 108.1 | |
| $p_8$ | ∠H−C−C | 110.0(4) | 111.3 | 0.5 | 111.5(3) | 111.2 | 0.5 |
| $p_9$ | $\phi$X−Si−C−C | 62.7(8) | 65.2 | 1.0 | 64.7(6) | 65.1 | 1.0 |
| $p_{10}$ | $\phi$X−Si−C−H(α) | 58.6(19) | 57.7 | 2.0 | 56.8(17) | 56.9 | 2.0 |
| $p_{11}$ | $\phi$X−Si−C−H($\beta$) | 173.3(18) | 172.3 | 2.0 | 171.9(16) | 172.4 | 2.0 |
| $p_{12}$ | $\phi$X−Si−C(27)−C(30) | 174.5(26) | 174.5 | 3.0 | 177.7(25) | 175.0 | 3.0 |
| $p_{13}$ | % conformer II | 57[b] | 41.1[c] | | 33[b] | 41.3[c] | |
| | | | Dependent | | | | |
| $p_{15}$ | ∠C(4)−Si−C(3)[II] | 112.1(1) | | | 111.5(1) | | |
| $p_{16}$ | ∠C(4)−Si−C(5)[II] | 112.0(1) | | | 111.5(1) | | |
| $p_{17}$ | ∠C(26)−Si−C(27)[IV] | 112.2(1) | 112.2 | | 111.6(1) | 112.3 | |
| $p_{18}$ | ∠C(26)−Si−C(28)[IV] | 112.2(1) | | | 111.7(1) | | |
| $p_{19}$ | ∠C(27)−Si−C(28)[IV] | 112.0(1) | | | 111.5(1) | | |

[a] Average values for conformers II and IV; taken as starting point for the GED refinement. [b] See text and Figures 5 and 6 for uncertainties in the amounts of conformers. [c] Calculated from theoretical values considering the presence of only the two main conformers in the sample.

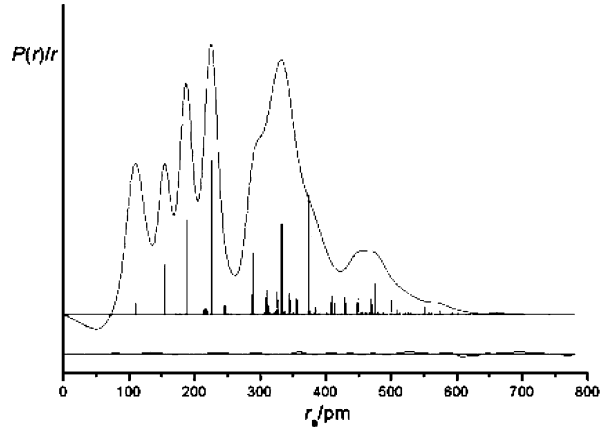


**Figure 4.** Experimental and difference (experimental − theoretical) radial-distribution curves $P(r)/r$ for TEBS. Before Fourier inversion, the data were multiplied by $s\cdot\exp(-0.00002s^2)/(Z_{Br} - f_{Br})(Z_C - f_C)$.

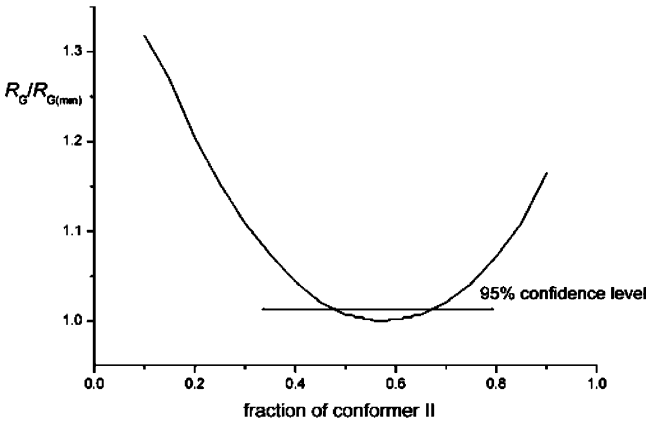


**Figure 5.** Variation in $R_G/R_{G(min)}$ with different amounts of conformer II for TECS.

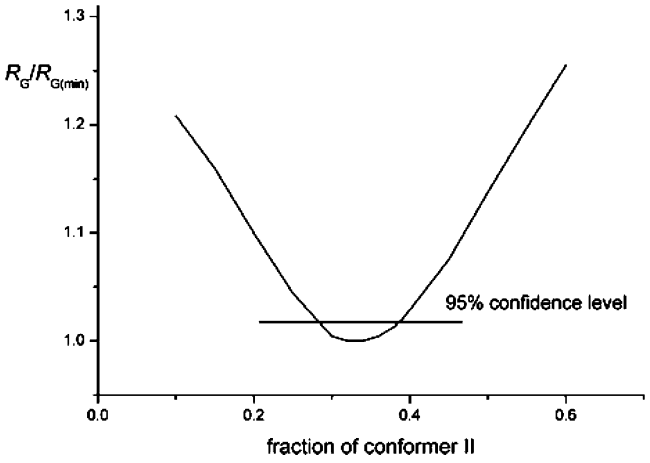


**Figure 6.** Variation in $R_G/R_{G(min)}$ with different amounts of conformer II for TEBS.

average of three methyl ∠H−C−C ($p_8$). The three dihedral angles common to the three conformers were $\phi$X−Si−C−C ($p_9$), $\phi$X−Si−C−H($\alpha$) ($p_{10}$), and $\phi$X−Si−C−H($\beta$) ($p_{11}$). (See Figure 2 for atom numbering and definitions of $\alpha$ and $\beta$.) Parameter 12, as described in the previous paragraph, is only found in conformer IV. In addition to the 12 geometric parameters, a proportionality parameter has been included to allow the relative amounts of each conformer to be changed. Parameter 13 controls the amount of conformer II considered to be part of the gas mixture. Initially, this parameter remained fixed at the amount calculated using the Boltzmann equation,

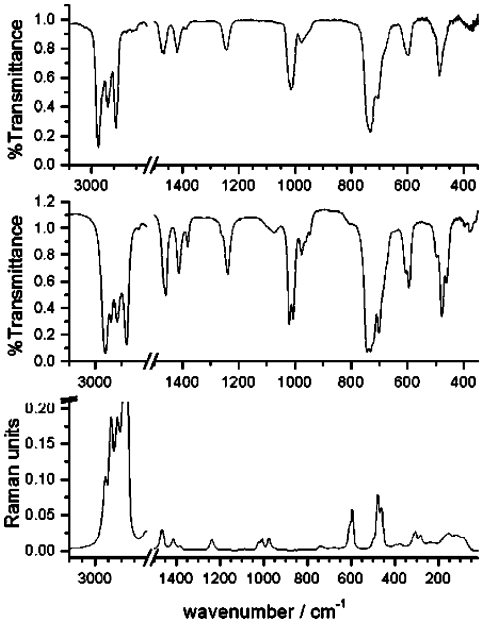


**Figure 7.** Experimental IR spectra of the gas phase (top) and the liquid phase (middle) and Raman spectrum of the liquid phase (bottom) for TECS.

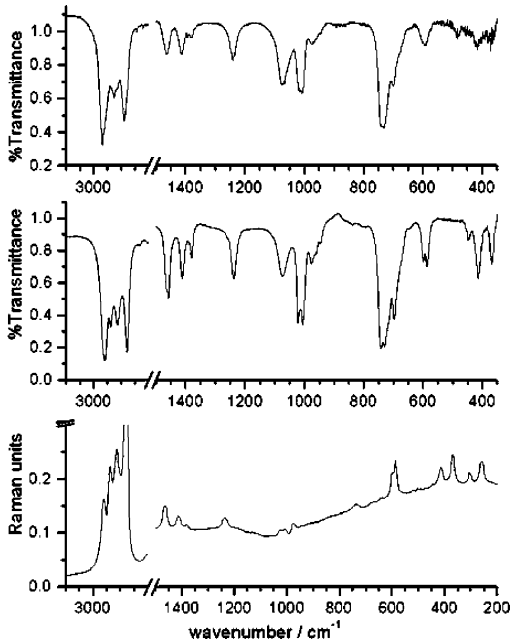


**Figure 8.** Experimental IR spectra of the gas phase (top) and the liquid phase (middle) and Raman spectrum of the liquid phase (bottom) for TEBS.

and only conformers II and IV (approximately 30% of conformer II and 40% of conformer IV, for both TECS and TEBS) were considered. Once the geometric parameters had been refined, $p_{13}$ was varied to find the experimental composition of each of the gases.

Of the 12 geometric parameters used to define the two-conformer model of TECS, six were restrained using the SARACEN method.[23] For the refinement of TEBS, five were restrained. In Table 3, the refined parameters for TECS and TEBS are reported and compared with their calculated MP2/aug-cc-pVDZ values. The C−Si−C angles are also included as dependent parameters. Additionally, eight groups of amplitudes of vibration were refined for both TECS and TEBS (no

**TABLE 4: Experimental and Calculated Frequencies (in cm$^{-1}$) of TECS**[a]

| theoretical/scaled B3LYP | | | | | | | |
|---|---|---|---|---|---|---|---|
| conformer II | | conformer IV | | experimental[b] | | | |
| 6-31G* | DZP+diff | 6-31G* | DZP+diff | IR gas | IR liquid | Raman liquid | P.E.D.[c] |
| 44 A″ | 47 A″ | 47 | 51 | | | | $\tau_{SiC}$ |
| 58 A′ | 64 A′ | 61 | 62 | | | | |
| 80 A″ | 87 A″ | 71 | 73 | | | | |
| 92 A′ | 92 A′ | 94 | 94 | | | | $\delta^a_{SiC3} + \rho_{SiC3} + sc_{SiC3}$ |
| 130 A′ | 129 A′ | 120 | 120 | | | 120 w,dp | $\rho_{SiC3}(sc_{SiC3})$ |
| 128 A″ | 135 A″ | 127 | 135 | | | | $\delta^s_{SiC3}$ |
| 152 A″ | 154 A″ | 151 | 154 | | | 154 w,dp | $\rho_{SiC3} + \delta^a_{SiC3}$ |
| 162 A′ | 162 A′ | 155 | 157 | | | | |
| 218 A″ | 219 A″ | 219 | 219 | | | | $\tau_{CC}(sc_{SiC3})$ |
| 234 A″ | 232 A″ | 233 | 232 | | | 235 w,p? | $\tau_{CC}$ |
| 234 A′ | 234 A′ | 238 | 238 | | | | |
| | | | | | | | $\tau_{CC} + \delta^s_{SiC3}$ |
| | | 277 | 279 | | | 282 w,p | **$sc_{SiC3} + \delta^a_{SiC3}$** |
| **299 A′** | **300 A′** | | | | | **305 w,p** | |
| **303 A′** | **308 A′** | | | | | | |
| | | | 318 | | | | |
| 360 A″ | 360 A″ | | | | | | |
| | | 381 | 380 | | 380 m | 378 vw | |
| | | | | | | **395 vw** | **$sc_{SiC3}$ (V)** |
| | | | | **458 sh** | **461 s** | **461 m,p** | **$\nu_{SiCl}$ (V)** |
| 481 A′ | 478 A′ | 477 | 476 | 486 s | 478 s | 476 m,p | $\nu_{SiCl}$ |
| | | | | **500 sh** | **497 m** | **500 sh** | **$\nu_{SiCl}$ (III)** |
| | | 592 | 594 | 600 s | 595 s | 594 m,p | **$\nu_{SiC}$** |
| **605 A′** | **607 A′** | | | | **606 s** | **608 m,p** | |
| 634 A″ | 634 A″ | 631 | 636 | | | | **$\rho_{CH2} + \nu_{SiC}$** |
| | | 673 | 673 | | 671 sh | | |
| **679 A″** | **680 A″** | | | | **686 sh** | | |
| 703 A′ | 706 A′ | 703 | 703 | 704 s | 701 s | | |
| **724 A″** | **722 A″** | | | **724 sh** | **719 sh** | | **$\rho_{CH2}$** |
| | | 730 | 730 | 732 vs | 732 vs | 733 w,dp | $\nu_{SiC} + \rho_{CH2}$ |
| 744 A′ | 744 A′ | 747 | 745 | 745 vs | 743 vs | 745 w,dp | |
| 937 A″ | 936 A″ | 939 | 942 | | 947 w | | $\rho_{CH3} + tw_{CH2}$ |
| | | 941 | 944 | | | | |
| 955 A″ | 955 A″ | 961 | 961 | | 964 sh | | $\rho_{CH3} + \nu_{CC}$ |
| 959 A′ | 960 A′ | 966 | 968 | | | | |
| 971 A′ | 970 A′ | | | | | | |
| 968 A″ | 971 A″ | 971 | 973 | 977 m | 975 m | 976 w,pp | $\nu_{CC} + tw_{CH2}$ |
| 974 A′ | 977 A′ | 975 | 979 | | | | |
| | | 1007 | 1005 | 1009 s | 1006 s | 1007 w,p | $\rho_{CH3} + \nu_{CC} + wa_{CH2}$ |
| 1013 A′ | 1011 A′ | 1018 | 1017 | 1013 s | | | $\nu_{CC} + \rho_{CH3}$ |
| 1014 A′ | 1011 A′ | | | | | | |
| 1037 A″ | 1033 A″ | 1028 | 1025 | 1023 s | 1021 s | 1022 w,p | |
| 1238 A″ | 1233 A″ | 1242 | 1238 | 1244 m | 1239 s | 1236 w,p | $tw_{CH2}$ |
| 1240 A″ | 1236 A″ | 1244 | 1240 | | | | |
| 1245 A′ | 1244 A′ | 1248 | 1245 | | | | |
| 1256 A′ | 1260 A′ | 1256 | 1258 | | 1261 sh | | $wa_{CH2}$ |
| 1259 A″ | 1261 A″ | 1257 | 1258 | | | | |
| 1262 A′ | 1265 A′ | 1262 | 1264 | | | | |
| 1385 A′ | 1383 A′ | 1379 | 1379 | 1385 w | 1380 m | 1381 w,p | $\delta^s_{CH3}$ |
| 1386 A″ | 1383 A″ | 1380 | 1381 | | | | |
| 1387 A′ | 1384 A′ | 1381 | 1381 | | | | |
| 1415 A″ | 1412 A″ | 1401 | 1405 | 1419 m | 1413 s | 1412 w,dp | $sc_{CH2}$ |
| 1421 A′ | 1419 A′ | 1418 | 1415 | | | | |
| 1425 A′ | 1422 A′ | 1423 | 1421 | | | | |
| 1456 A′ | 1455 A′ | 1455 | 1455 | 1465 m | 1459 s | 1464 w,dp | $\delta^a_{CH3}$ |
| 1458 A″ | 1457 A″ | 1457 | 1458 | | | | |
| 1459 A′ | 1459 A′ | 1458 | 1459 | | | | |
| 1461 A″ | 1460 A″ | 1460 | 1461 | | | | |
| 1463 A′ | 1462 A′ | 1462 | 1462 | | | | |
| 1463 A″ | 1463 A″ | 1463 | 1463 | | | | |
| 2871 A″ | 2872 A″ | 2873 | 2874 | 2890 vs | 2880 vs | 2881 s,p | $\nu^s_{CH2}$ |
| 2875 A′ | 2875 A′ | 2875 | 2876 | | | | |
| 2881 A′ | 2878 A′ | 2884 | 2882 | | | | $\nu^s_{CH3}$ |
| 2885 A″ | 2881 A″ | 2887 | 2885 | | | | |
| 2885 A′ | 2882 A′ | 2888 | 2886 | | | | |
| 2895 A′ | 2896 A′ | 2894 | 2894 | | | | $\nu^a_{CH2}$ |
| 2912 A″ | 2914 A″ | 2910 | 2914 | 2926 s | 2915 s | 2914 s,p | |
| 2915 A′ | 2918 A′ | 2915 | 2919 | | | | |
| 2925 A″ | 2928 A″ | 2922 | 2925 | | | | |
| 2940 A′ | 2942 A′ | 2938 | 2942 | | 2939 s | 2939 s,p | $\nu^a_{CH3}$ |

**TABLE 4: Continued**

| theoretical/scaled B3LYP | | | | experimental[b] | | | |
|---|---|---|---|---|---|---|---|
| conformer II | | conformer IV | | | | | |
| 6-31G* | DZP+diff | 6-31G* | DZP+diff | IR gas | IR liquid | Raman liquid | P.E.D.[c] |
| 2941 A″ | 2943 A″ | 2938 | 2943 | | | | |
| 2941 A′ | 2944 A′ | 2940 | 2944 | | | | |
| 2947 A″ | 2948 A″ | 2946 | 2948 | | | | |
| 2956 A″ | 2955 A″ | 2955 | 2955 | 2968 vs | 2961 vs | 2960 vs,dp | |
| 2957 A′ | 2956 A′ | 2955 | 2956 | | | | |

[a] Calculations were performed at the B3LYP level using the 6-31G* and DZP+diff basis sets for the three main conformers. The symmetry of each mode in conformer II is shown next to its calculated values. For conformer IV, all modes have A symmetry. The main terms of the PED for each mode are also shown. Bands that demonstrate the presence of different conformers are shown in bold. [b] Abbreviations used: vs = very strong, s = strong, m = medium, w = weak, vw = very weak, p = polarized, dp = depolarized, pp = partially polarized. [c] Abbreviations and Greek symbols (in order of appearance): $\tau$ = torsion, $\delta$ = deformation, $\rho$ = rocking, sc = scissoring, $\nu$ = stretching, tw = twisting, wa = wagging. The superscripts a and s denote asymmetric and symmetric, respectively.

restraints were required). Tables S5 and S6 (Supporting Information) list the amplitudes of vibration for TECS and TEBS, respectively.

The success of the GED refinements can be gauged visually using Figures 3 and 4, where the radial-distribution curves and the theoretical minus experimental difference curves for TECS and TEBS are shown. The lines under the peaks in the radial-distribution curves represent individual interatomic distances, with the relative heights of the sticks proportional to the atomic numbers of the atoms involved and to the multiplicity of that distance and inversely proportional to the magnitude of the distance itself. The success of a refinement can also be quantified from the value of the goodness-of-fit function, $R_G$. For both TECS and TEBS, these values are low: 0.043 for TECS and 0.044 for TEBS. For TECS, the best fit relates to a composition of 57% conformer II and 43% conformer IV. For TEBS, these compositions were 33% conformer II and 67% of conformer IV. These results are in relatively good agreement with those obtained from the Boltzmann distributions at the experimental temperatures.

Figures 5 and 6 show the $R_G/R_{G(min)}$ variations with respect to the composition of the sample as the amount of each conformer was changed. To quantify the uncertainties associated with these experimental compositions, lines have been drawn through the curves at $R_G/R_{G(min)} = 1.016$, which, from Hamilton's tables,[24] represents a 95% confidence limit. The experimental mixtures for TECS and TEBS are therefore within two standard deviation of the calculated mixtures, albeit in different directions. Of course, there would also be small amounts of the other three conformers so the indicated uncertainties must be underestimates.

For further details of the refinement procedure, the least-squares correlation matrices are given in Tables S7 and S8 (Supporting Information), and the GED atomic coordinates for each conformer of both TECS and TEBS are reported in Tables S9 and S10. Finally, the molecular scattering intensities curves are shown in Figures S2 and S3.

**Vibrational Study.** The IR spectra of the gas and liquid phases and the Raman spectrum of the liquid phase have been recorded for TECS and TEBS and are shown in Figures 7 and 8, respectively. As explained in previous sections, two different basis sets have been used for the vibrational analyses, in conjunction with the B3LYP functional. The calculated geometries at these levels (reported in Tables S3 and S4) are close to those determined by experiment for both compounds (see Table 3) and, therefore, no empirical corrections have been made to the calculated geometries.

The vibrational frequencies calculated theoretically at the B3LYP level with the 6-31G* and DZP+diff basis sets have been fitted to the observed IR and Raman frequencies by means of a root-mean-squares procedure following the SQMFF methodology.[19−21] As explained in Computational Details, the scaling factors associated with the force constants, expressed in the set of natural coordinates defined for the TECS and TEBS molecules, were refined in order to reproduce the experimental frequencies, giving theoretical support to our proposal of vibrational assignment.

For the vibrational study, conformer IV has been used as a reference, since it is predicted to be the main conformer for both TECS and TEBS. The refined scaling factors obtained for this conformer were then transferred to the other four conformers, in order to predict their vibrational spectra. Using the scaled frequencies calculated for the two main conformers, we found it possible to explain almost all of the experimental features observed in the vibrational spectra. Some exceptions, which take into consideration conformers III and V, which are also predicted to be present in the sample in reasonable amounts, will be explained below. The scaled frequencies for the two main conformers at both levels of calculation, the experimental frequencies with their relative intensities, the proposed vibrational assignment, and the main terms of the PED are reported in Tables 4 and 5 for TECS and TEBS, respectively.

For clarity, and unless otherwise stated, throughout this discussion, we will refer to the B3LYP/DZP+diff results and the experimental bands observed in the IR spectra of the liquid phase. The latter can be justified by the small differences observed between the experimental gas and liquid frequencies and by the higher number of bands observed in the liquid phase, including those from Raman. Additionally, this strategy has given good results in previous studies with related systems.[3−6] The discussion below will concentrate on the parts of the vibrational spectra that cannot be explained if we consider only the presence of the main conformer. For the rest of the vibrational spectra, the scaled frequencies for the different conformers are almost identical. Complete vibrational assignments of the whole spectra have been accomplished for TECS and TEBS, as shown in Tables 4 and 5, respectively.

*Triethylchlorosilane.* The first evidence of the presence of different conformers of TECS, even in the liquid phase, is the weak polarized band observed at 305 $cm^{-1}$ in the Raman spectrum. That band, which cannot be assigned to conformer IV, is thus assigned to conformer II. This, in agreement with the results of the scaling, gives two normal modes at 300 and 308 $cm^{-1}$ (both belonging to the A′ irreducible representation of the $C_s$ symmetry group) describing the scissoring of the $SiC_3$ group. Moreover, a very weak band at 395 $cm^{-1}$ in the Raman spectrum cannot be assigned to any of the main conformers but can be assigned as the scissoring of the $SiC_3$ group in

**TABLE 5: Experimental and Calculated Frequencies (in cm$^{-1}$) of TEBS[a]**

| theoretical/scaled B3LYP | | | | | | | |
|---|---|---|---|---|---|---|---|
| conformer II | | conformer IV | | experimental[b] | | | |
| 6-31G* | DZP+diff | 6-31G* | DZP+diff | IR gas | IR liquid | Raman liquid | P.E.D.[c] |
| 48 A″ | 47 A″ | 53 | 54 | | | | $\tau_{SiC}$ |
| 57 A′ | 60 A′ | 59 | 61 | | | | |
| 80 A″ | 77 A″ | 75 | 72 | | | | |
| 87 A′ | 85 A′ | 92 | 89 | | | | $\delta^{a}_{SiC3}+\rho_{SiC3}+sc_{SiC3}$ |
| 119 A′ | 114 A′ | 110 | 108 | | | | $\rho_{SiC3}$ ($sc_{SiC3}$) |
| 122 A″ | 129 A″ | 127 | 132 | | | | $\delta^{s}_{SiC3}$ |
| 155 A′ | 151 A′ | 151 | 147 | | | | $\delta^{a}_{SiC3}+\rho_{SiC3}$ |
| 157 A″ | 155 A″ | 154 | 155 | | | | |
| 222 A″ | 219 A″ | 221 | 220 | | | | $\tau_{CC}$ ($sc_{SiC3}$) |
| 234 A′ | 231 A′ | 235 | 230 | | | | $\tau_{CC}$ |
| 238 A″ | 232 A″ | 240 | 237 | | | | |
| 262 A′ | 264 A′ | 252 | 253 | | | 259 w | $\nu_{SiBr}+sc_{SiC3}$ |
| 300 A′ | 302 A′ | 301 | 303 | | | 305 w | $sc_{SiC3}+\nu_{SiBr}$ |
| 356 A″ | 359 A″ | 368 | 368 | | 368 m | 368 m | $sc_{SiC3}+\nu_{SiBr}$ |
| 413 A′ | 409 A′ | 418 | 418 | | 415 s | 413 m | $\nu_{SiBr}$ |
| | | | | | **450 w** | | **$\nu_{SiBr}$ (III)** |
| | | 585 | 586 | 594 m,br | 586 m | 586 m | **$\nu_{SiC}$** |
| **599 A′** | **598 A′** | | | | **599 m** | **596 m** | |
| 634 A″ | 634 A″ | 634 | 636 | | | | $\rho_{CH2}+\nu_{SiC}$ |
| 681 A″ | 680 A″ | 674 | 672 | | | | |
| 705 A′ | 704 A′ | 699 | 700 | 700 s | 697 vs | 699 vw | |
| **724 A″** | **721 A″** | | | | **713 sh** | | **$\rho_{CH2}$** |
| | | 729 | 729 | 735 vs,br | 730 vs | 731 vw | $\nu_{SiC}+\rho_{CH2}$ |
| 742 A′ | 741 A′ | 743 | 743 | | 742 vs | | |
| 933 A″ | 937 A″ | 937 | 942 | 945 sh | 946 w | | $\rho_{CH3}+tw_{CH2}$ |
| | | 940 | 944 | | | | |
| 952 A″ | 955 A″ | 958 | 962 | | 962 m | | $\rho_{CH3}$ |
| 957 A′ | 960 A′ | 969 | 969 | | | | |
| 965 A′ | 969 A′ | | | | | | |
| 971 A″ | 972 A″ | 973 | 975 | 975 m | 977 m | 974 vw,p | $\nu_{CC}+\rho_{CH3}$ |
| 972 A′ | 978 A′ | 978 | 980 | | | | |
| 1011 A′ | 1011 A′ | 1007 | 1007 | 1008 s | 1006 s | 1005 vw,p | |
| 1014 A″ | 1013 A″ | | | | | | |
| 1027 A′ | 1036 A′ | 1020 | 1020 | 1015 s | 1022 s | 1024 vw,p | |
| | | 1030 | 1028 | | | | |
| 1236 A″ | 1233 A″ | 1245 | 1237 | 1241 s | 1238 s | 1236 vw | $tw_{CH2}$ |
| 1240 A″ | 1235 A″ | 1247 | 1239 | | | | |
| 1242 A′ | 1243 A′ | 1247 | 1244 | | | | |
| 1253 A′ | 1259 A′ | 1254 | 1257 | | 1261 sh | | $wa_{CH2}$ |
| 1255 A″ | 1260 A″ | 1256 | 1258 | | | | |
| 1259 A′ | 1264 A′ | 1261 | 1263 | | | | |
| 1384 A′ | 1382 A′ | 1380 | 1379 | 1381 w | 1380 w | 1381 vw | $\delta^{s}_{CH3}$ |
| 1386 A″ | 1383 A″ | 1381 | 1380 | | | | |
| 1386 A′ | 1384 A′ | 1382 | 1381 | | | | |
| 1416 A″ | 1411 A″ | 1401 | 1405 | 1414 m | 1412 m | 1412 w,dp | $sc_{CH2}$ |
| 1422 A′ | 1418 A′ | 1416 | 1412 | | | | |
| 1427 A′ | 1421 A′ | 1423 | 1419 | | | | |
| 1455 A′ | 1454 A′ | 1454 | 1453 | 1465 br | 1457 s | 1462 w,dp | $\delta^{as}_{CH3}$ |
| 1458 A″ | 1456 A″ | 1457 | 1455 | | | | |
| 1460 A′ | 1458 A′ | 1457 | 1456 | | | | |
| 1460 A″ | 1459 A″ | 1460 | 1458 | | | | |
| 1462 A′ | 1460 A′ | 1460 | 1459 | | | | |
| 1464 A″ | 1461 A″ | 1462 | 1461 | | | | |
| 2871 A′ | 2868 A′ | 2871 | 2868 | 2889 vs | 2878 vs | 2879 vs,p | $\nu^{s}_{CH2}$ |
| 2874 A′ | 2871 A′ | 2874 | 2871 | | | | |
| 2881 A″ | 2876 A″ | 2884 | 2879 | | | | $\nu^{s}_{CH3}$ |
| 2884 A′ | 2880 A′ | 2887 | 2882 | | | | |
| 2885 A′ | 2881 A′ | 2888 | 2883 | | | | |
| 2897 A″ | 2896 A″ | 2895 | 2893 | | | | $\nu^{a}_{CH2}$ |
| 2914 A′ | 2913 A′ | 2911 | 2912 | 2925 s | | | |
| 2917 A′ | 2917 A′ | 2916 | 2917 | | | | |
| 2928 A″ | 2928 A″ | 2923 | 2924 | | | | |
| 2939 A′ | 2941 A′ | 2937 | 2938 | | 2938 vs | 2937 s,p | $\nu^{a}_{CH3}$ |
| 2941 A″ | 2941 A″ | 2939 | 2940 | | | | |
| 2942 A′ | 2942 A′ | 2940 | 2941 | | | | |
| 2948 A″ | 2947 A″ | 2947 | 2946 | | | | |
| 2955 A″ | 2954 A″ | 2953 | 2952 | 2968 vs | 2960 vs | 2960 s,p | |
| 2955 A′ | 2955 A′ | 2954 | 2953 | | | | |

[a] Calculations were performed at the B3LYP level using the 6-31G* and DZP+diff basis sets for the three main conformers. The symmetry of each mode in conformer II is shown next to its calculated values. For conformer IV, all modes have A symmetry. The main terms of the PED for each mode are also shown. Bands that demonstrate the presence of different conformers are shown in bold. [b] Abbreviations used: vs = very strong, s = strong, m = medium, w = weak, vw = very weak, p = polarized, dp = depolarized, pp = partially polarized. [c] Abbreviations and Greek symbols (in order of appearance): $\tau$ = torsion, $\delta$ = deformation, $\rho$ = rocking, sc = scissoring, $\nu$ = stretching, tw = twisting, wa = wagging. The superscripts a and s denote asymmetric and symmetric, respectively.

**TABLE 6: Scaling Factors Obtained for Both Triethylsilyl Derivatives**

| scaling factor | B3LYP/6-31G* | | | B3LYP/DZP+diff | | |
|---|---|---|---|---|---|---|
| | TECS | TEBS | average | TECS | TEBS | average |
| SiC | 1.031 | 1.022 | 1.026 | 1.019 | 1.016 | 1.017 |
| CC | 0.942 | 0.956 | 0.949 | 0.962 | 0.966 | 0.964 |
| CH (=$CH_2$) | 0.906 | 0.905 | 0.905 | 0.910 | 0.908 | 0.909 |
| CH (−$CH_3$) | 0.897 | 0.897 | 0.897 | 0.903 | 0.901 | 0.902 |
| $CH_2$ sc. | 0.916 | 0.913 | 0.914 | 0.959 | 0.957 | 0.958 |
| $SiC_3$ sc. | 1.064 | 1.064 | 1.064 | 1.071 | 1.107 | 1.089 |
| $CH_2$ rock | 0.947 | 0.951 | 0.949 | 0.963 | 0.970 | 0.966 |
| $CH_2$ wag | 0.937 | 0.936 | 0.936 | 0.982 | 0.985 | 0.984 |
| $CH_2$ tw. | 0.925 | 0.951 | 0.938 | 0.982 | 0.975 | 0.978 |
| sym. $CH_3$ def. | 0.924 | 0.925 | 0.924 | 0.963 | 0.963 | 0.963 |
| asym. $CH_3$ def. | 0.899 | 0.899 | 0.899 | 0.946 | 0.942 | 0.944 |
| $CH_3$ rock | 0.973 | 0.957 | 0.965 | 0.975 | 0.982 | 0.979 |
| sym. $SiC_3$ def. | 0.768 | 0.768[a] | 0.768 | 0.894 | 0.894[a] | 0.894 |
| asym. $SiC_3$ def. | 0.965 | 0.965[a] | 0.965 | 0.907 | 0.907[a] | 0.907 |
| $SiC_3$ rock | 0.736 | 0.736[a] | 0.736 | 0.714 | 0.714[a] | 0.714 |
| SiC torsion | 1.000 | 1.000 | 1.000[b] | 1.000 | 1.000 | 1.000[b] |
| CC torsion | 0.905 | 0.905[a] | 0.905 | 0.995 | 0.995[a] | 0.995 |

[a] These values were transferred from TECS, since there were no experimental bands for this region in the TEBS spectra. [b] Not refined because of the lack of experimental data.

conformer V, which agrees with the value calculated after the scaling of the force fields, that is, 400 $cm^{-1}$.

In the spectral region where the Si−Cl stretch appears, three bands are observed where only one would have been expected if there were just one conformer present. These bands appear at 461 $cm^{-1}$, 478 $cm^{-1}$, and 497 $cm^{-1}$. The first is assigned as the SiCl stretching in conformer V (calculated at 457 $cm^{-1}$). The second band is assigned to conformers II and IV, for which the calculated values are very close to one another and close to the observed value, 478 $cm^{-1}$ (A′) in conformer II and 476 $cm^{-1}$ in conformer IV. The third band in that region is assigned to conformer III, for which the SiCl stretching normal mode is calculated to be at 502 $cm^{-1}$.

At 606 $cm^{-1}$, there is one strong band, which cannot be assigned to the main conformer. It is, therefore, assigned to conformer II in accordance with the calculated value for its SiC stretching normal mode, that is, 607 $cm^{-1}$ (A′). Similarly, the shoulder observed at 686 $cm^{-1}$ in the IR spectrum of the liquid is assigned to conformer II, which corresponds to a normal mode calculated at 680 $cm^{-1}$ with contributions from the $CH_2$ rocking and the SiC stretching vibrations.

Finally, another shoulder at 719 $cm^{-1}$ in the IR spectrum of the liquid (724 $cm^{-1}$ in the gas), which cannot be assigned to the main conformer, is assigned to the $CH_2$ rocking mode of conformer II, in agreement with its calculated value of 722 $cm^{-1}$ (A″). As can be seen in Table 4, where the whole assignment is shown, the remaining bands can be assigned to conformer IV, and in the majority of the cases the scaled frequencies for the two main conformers are calculated to be very close.

*Triethylbromosilane.* In TEBS, the first evidence of the presence of more than one conformer is the weak band observed in the IR spectrum of the liquid phase at 450 $cm^{-1}$, which is assigned to the SiBr stretching normal mode of conformer III, in agreement with its calculated value, 451 $cm^{-1}$. This assignment is similar to that of the SiCl stretching mode in TECS, in which the band appearing in that region at a higher frequency was also assigned to conformer III. At higher frequencies, we observed two bands where only one was expected. The first, at 586 $cm^{-1}$, is assigned to the SiC stretching normal mode of conformer IV (calculated at 586 $cm^{-1}$), whereas the other band, observed at 599 $cm^{-1}$, is assigned to the SiC stretch of conformer II, in accordance with its calculated value, 598 $cm^{-1}$ (A′). This assignment also agrees with that for TECS.

The last band that cannot be assigned to the main conformer is the shoulder at 713 $cm^{-1}$. Once again, the proposed assignment is similar to that in TECS. The band has been assigned to conformer II, in accordance with the calculated value for the $CH_2$ rocking in this conformer, that is, 721 $cm^{-1}$ (A″). In Table 5, the results for the whole vibrational assignment are shown and, as can be seen, the scaled frequencies for the two main conformers have very similar values and are in good agreement with the experimental bands.

In Table 6, the scaling factors obtained after the refinement procedure for TECS and TEBS, at the two levels employed, are reported. The values for TECS and TEBS are in good accordance, and so it is possible to average them, obtaining a set of parameters for each basis set.

## Conclusions

It has been demonstrated that five different conformers represent minima on the PES of the title molecules. Theoretical analyses of the gas phase populations in terms of the Boltzmann distribution using $\Delta G$ values calculated using the B3LYP and MP2 methods with the 6-31G*, DZP+diff, and aug-cc-pVDZ basis sets indicated that conformer II ($C_s$) and conformer IV ($C_1$) account for around 70% of the sample composition.

The structures of TECS and TEBS have been determined experimentally by GED. For each, a model involving the two main conformers was used for the refinement of the experimental data. For TECS, the lowest $R_G$ value was for a composition of 57% of conformer II and 43% of conformer IV, and for TEBS, the best fit represented 33% of conformer II and 67% of conformer IV, which are in good agreement with the results from the theoretical calculations.

The vibrational spectra of both TECS and TEBS have been completely assigned, following similar patterns in both compounds. The proposed assignment includes bands that could only be explained by considering the presence of more than one conformer. Although the majority of the bands could be explained by taking into account only the contributions from conformers II and IV, assignments of some bands used the scaled frequencies predicted for the remaining conformers, specifically, conformers III and V. Additionally, the use of the SQMFF methodology has allowed us to obtain two sets of scaling factors, one for each basis set used for the vibrational assignment. These parameters could, in the future, be transferred to other more reactive or unstable alkylsilane derivatives, such as silicon alkoxides or silanols, which take part in sol−gel processes of industrial interest, in order to predict their vibrational spectra. These data could be used in the monitoring of these processes, for which IR and Raman techniques have proved themselves to be very powerful tools.

**Acknowledgment.** M.M. thanks Fundación Ramón Areces for funding a Ph.D. studentship supporting this work. M.M., F.P.U., F.M., and J.J.L.G. acknowledge Prof. Tom Sundius for allowing us to use MOLVIB and also acknowledge Francisco Hermoso for his help in recording the spectra. D.A.W. is currently funded by the EPSRC, who also fund the electron diffraction research (Grant EP/C513649). Financial support from the MEC-FEDER Spanish project (CTQ2006-11306/BQU) and the Andalusian Government (FQM-173) is gratefully acknowledged by M.M.G., F.P.U., F.M., and J.J.L.G.

**Supporting Information Available:** Detailed information is available on the electron diffraction experiment (Table S1),

the natural-coordinate system employed (Table S2 and Figure S1), bond lengths, angles and torsions calculated at the MP2 and B3LYP levels (Tables S3 and S4), amplitudes of vibration from the GED experiment (Tables S5 and S6), correlation matrices from the least-squares refinements (Tables S7 and S8), coordinates from the GED structures (Tables S9 and S10), and molecular scattering intensity curves (Figures S2 and S3). This material is available free of charge via the Internet at http://pubs.acs.org.

## References and Notes

(1) Kunai, A.; Oshita, J. *J. Organomet. Chem.* **2003**, *686*, 3, and references therein. Denmark, S. E.; Ober, M. H. *Aldrichim. Acta* **2003**, *36*, 75, and references therein. Herzog, U. In *Chemistry of Organic Silicon Compounds;* Rappoport, Z, Apeloig, Y., Eds.; John Wiley and Sons: Chichester, U.K., 2001; Vol. 3, pp 469−489, and references therein.

(2) Brinker, C. J.; Scherer, G. W. *Sol-Gel Science: The Physics and Chemistry of Sol-Gel Processing;* Academic Press: San Diego, CA, 1989.

(3) Montejo, M.; Partal, F.; Márquez, F.; Ignatyev, I. S.; López González, J. J. *Spectrochim. Acta A* **2005**, *62*, 293.

(4) Montejo, M.; Partal, F.; Márquez, F.; Ignatyev, I. S.; López González, J. J. *J. Mol. Struct.* **2005**, *331*, 744.

(5) Montejo, M.; Partal, F.; Márquez, F.; López González, J. J. *Spectrochim. Acta A* **2005**, *62*, 1058.

(6) Montejo, M.; Hinchley, S. L.; Ben Altabef, A.; Robertson, H. E.; Partal, F.; Rankin, D. W. H.; López González, J. J. *Phys. Chem. Chem. Phys.* **2006**, *8*, 477.

(7) Dernova, V. S. Main parameters of Raman lines and infrared absorption bands in vibrational spectra of triethylchlorosilane. *Spektroskopich. Svoistva Soedin. Elementov IV B Gruppy;* Saratov, U.S.S.R., 1981; pp 10−14.

(8) Ryskin, Ya. I.; Voronkov, M. G. *Collect. Czech. Chem. Commun.* **1959**, *24*, 3816.

(9) Volkov, V. F.; Vyshinskii, N. N.; Rudnevskii, N. K. *Izv. Ross. Akad. Nauk, Ser. Fiz.* **1962**, *26*, 1282.

(10) Huntley, C. M.; Laurenson, G. S.; Rankin, D. W. H. *J. Chem. Soc., Dalton Trans.* **1980**, 954.

(11) Hinchley, S. L.; Robertson, H. E.; Borisenko, K. B.; Turner, A. R.; Johnston, B. F.; Rankin, D. W. H.; Ahmadian, M.; Jones, J. N.; Cowley, A. H. *Dalton Trans.* **2004**, 2469.

(12) Fleischer, H.; Wann, D. A.; Hinchley, S. L.; Borisenko, K. B.; Lewis, J. R.; Mawhorter, R. J.; Robertson, H. E.; Rankin, D. W. H. *Dalton Trans.* **2005**, 3221.

(13) Ross, A. W.; Fink, M.; Hilderbrandt, R. In *International Tables for Crystallography;* Wilson, A. J. C., Ed.; Kluwer Academic Publishers: Dordrecht, The Netherlands, 1992; Vol. C, p 245.

(14) Frisch, M. J.; Trucks, G. W.; Schlegel, H. B.; Scuseria, G. E.; Robb, M. A.; Cheeseman, J. R.; Montgomery, J. A., Jr.; Vreven, T.; Kudin, K. N.; Burant, J. C.; Millam, J. M.; Iyengar, S. S.; Tomasi, J.; Barone, V.; Mennucci, B.; Cossi, M.; Scalmani, G.; Rega, N.; Petersson, G. A.; Nakatsuji, H.; Hada, M.; Ehara, M.; Toyota, K.; Fukuda, R.; Hasegawa, J.; Ishida, M.; Nakajima, T.; Honda, Y.; Kitao, O.; Nakai, H.; Klene, M.; Li, X.; Knox, J. E.; Hratchian, H. P.; Cross, J. B.; Bakken, V.; Adamo, C.; Jaramillo, J.; Gomperts, R.; Stratmann, R. E.; Yazyev, O.; Austin, A. J.; Cammi, R.; Pomelli, C.; Ochterski, J. W.; Ayala, P. Y.; Morokuma, K.; Voth, G. A.; Salvador, P.; Dannenberg, J. J.; Zakrzewski, V. G.; Dapprich, S.; Daniels, A. D.; Strain, M. C.; Farkas, O.; Malick, D. K.; Rabuck, A. D.; Raghavachari, K.; Foresman, J. B.; Ortiz, J. V.; Cui, Q.; Baboul, A. G.; Clifford, S.; Cioslowski, J.; Stefanov, B. B.; Liu, G.; Liashenko, A.; Piskorz, P.; Komaromi, I.; Martin, R. L.; Fox, D. J.; Keith, T.; Al-Laham, M. A.; Peng, C. Y.; Nanayakkara, A.; Challacombe, M.; Gill, P. M. W.; Johnson, B.; Chen, W.; Wong, M. W.; Gonzalez, C.; Pople, J. A. *Gaussian 03*, revision C.01; Gaussian, Inc.: Wallingford, CT, 2004.

(15) Hehre, W. J.; Random, L.; Schleyer, P. v. R.; Pople, J. A. *Ab Initio Molecular Orbital Theory;* Wiley: New York, 1986.

(16) Ignatyev, I. S.; Partal, F.; López González, J. J. *J. Phys. Chem. A* **2002**, *106*, 11644.

(17) Dunning, T. H. *J. Chem. Phys.* **1989**, *90*, 1007. Kendall, R. A.; Dunning, T. H.; Harrison, R. J. *J. Chem. Phys.* **1992**, *90*, 6796.

(18) Sipachev, V. A. *J. Mol. Struct.* (*THEOCHEM*) **1985**, *121*, 143.

(19) Fogarasi, G.; Pulay, P. In *Vibrational Spectra and Structure;* Durig, J. R., Ed.; Elsevier: Amsterdam, The Netherlands, 1985; Vol. 14, p 125.

(20) Rauhut, G.; Pulay, P. *J. Phys. Chem. A* **1995**, *99*, 3093.

(21) Fogarasi, G.; Zhou, X.; Taylor, P. W.; Pulay, P. *J. Am. Chem. Soc.* **1992**, *114*, 8191.

(22) Sundius, T. *J. Mol. Struct.* **1990**, *218*, 321. Sundius, T. *Vib. Spectrosc.* **2002**, *29*, 89.

(23) Brain, P. T.; Morrison, C. A.; Parsons, S.; Rankin, D. W. H. *J. Chem. Soc., Dalton Trans.* **1996**, 4589. Blake, A. J.; Brain, P. T.; McNab, H.; Miller, J.; Morrison, C. A.; Parsons, S.; Rankin, D. W. H.; Robertson, H. E.; Smart, B. A. *J. Phys. Chem. A* **1996**, *100*, 12280. Mitzel, N. W.; Rankin, D. W. H. *Dalton Trans.* **2003**, 3650.

(24) Hamilton, W. C. *Acta Cryst.* **1965**, *18*, 502.